Modeling and Control of a Grid-Connected PV Energy Conversion System

HAMID OUATMAN
Mohammadia High School
Department of Electrical Engineering
RABAT, MOROCCO
h.ouatman@mem.gov.ma

MOHAMMED OUASSAID
Cady Ayyad University
Department of Electrical Engineering
MARRAKECH, MOROCCO
ouassaid@yahoo.fr

MOHAMED CHERKAOUI
Mohammadia High School
Department of Electrical Engineering
RABAT, MOROCCO
cherkaoui@emi.ac.ma

Abstract : This paper investigates the efficiency of the Photovoltaic (PV) array. The proposed model is based on a DC-DC boost converter and a three-phase grid connected DC-AC inverter. This structure is used to provide the flexibility of the system and the quality of the generated waves. In order to improve the efficiency of the Photovoltaic array, a Maximum Power Point Tracking (MPPT) is used to provide a good results if the converter is controlled with PID compensator. The control of the output voltage is provided by the Pulse Width Modulation (PWM) technique. The three-level Voltage Source Converter (VSC) regulates DC bus voltage and keeps unity power factor. The results are presented in this paper using Matlab/simulink, which validate the pracicability of the proposed system.

Key–Words : PV System, MPPT, PID Compensator, Boost converter, PLL, Unity Power Factor, Three-level VSC

1 Introduction

With plenty of energy emitted by the sun, solar energy is an important alternative and increasingly source of the electricity production. Using photovoltaic system, we can directly convert the energy carried by the solar rays into electricity. For their simplicity of implementation, lack of fuel cost and noise, currently the production of electricity by photovoltaic systems is considered as an important source for the production of electricity. These power generation systems assume a quality of energy, flexibility and cost effectiveness. Also, the control voltage, the correction of the power factor and harmonic filtering should be provided.[1, 2]

There have been many investigations reported on the control of the boost converter in literature [3, 4]. To enhance the cost effectiveness of the system we proposed to use MPPT technique and PID compensator. Therefore, the purpose of this paper is the modeling and control of a grid-connected PV energy conversion system using DC-DC and DC-AC converters. These converters should allow optimum transfer of energy produced with quality waves generated by the photovoltaic generator. This paper is organized as follows. Section 2 describes the modeling of the PV array. Section 3 introduces the modeling and control of DC-DC Boost converter. in Section 4, the command and control of DC-AC converter and network interface. Then, the obtained results using Matlab/Simulink are discussed in Section 5. Finally, conclusions are drawn in Section 6.

2 Modeling of the photovoltaic array

A basic photovoltaic cell is a low-power electric generator. To simplify the behavior of a real photovoltaic cell we proposed to use the model of a cell with a single diode, figure 1. This model has almost the same accuracy that gives the model with two diodes in parallel. [4, 5]
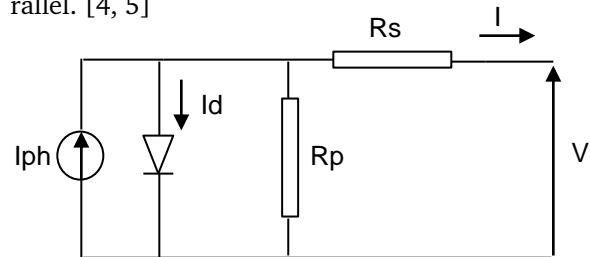

Fig.1. Equivalent circuit of a real solar cell

A solar cell can be described by the following equations for the model with the single diode :

$$I = I_{ph} - I_{sat}[exp(\frac{V + R_s I}{a V_t})] - \frac{V + R_s I}{R_p} \qquad (1)$$

Where I_{sat} is the reverse saturation current of the diode, a is non-ideality factor of the p-n junction, $V_t = \frac{q}{KT}$, R_p and R_s are the intrinsic shunt and series resistance of the solar cell respectively, I_{ph} is the generated current under a given irradiation and I and V are the output current and output voltage of the PV cell.

The single diode model has been simulated using the Matlab/Simulink. The curve of figure 2 shows
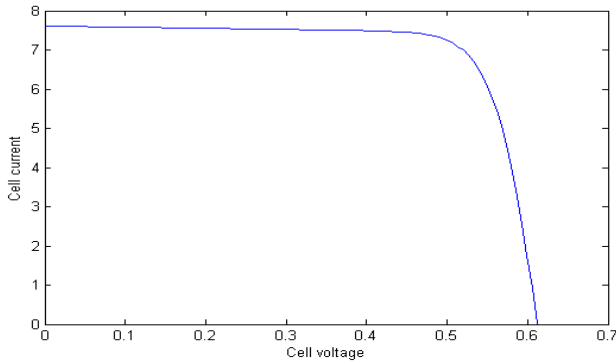
Fig.2. Current-voltage of a photovoltaic cell.

Fig.4. Current-voltage characteristic of the photovoltaic module.

the current-voltage I(V) of a photovoltaic cell. indeed, photovoltaic modules are made by series association in order increase the voltage of the PV generator and / or in parallel in order increase the output current of the generator [6, 7]. A module consists of N_s cells in series and in parallel N_p cells, the equation of photo-generated current I_{ph} in Standard Test Conditions ($G = 1000W/m^2$ and $T_a = 25C, AM1.5$) is given by :

$$I_{ph} = (I_{ph,n} + K_I \Delta(T)) \frac{G}{G_n} \qquad (2)$$

The conduction current of the diode is given by the following equation :

$$I_d = I_{sat}[exp(\frac{V + R_s I}{aV_t}) - 1] \qquad (3)$$

The saturation current of the diode is given by the following equation :

$$I_{sat} = \frac{I_{sc,n} + K_I \Delta(T)}{[exp(\frac{V_{oc,n} + K_V \Delta(T)}{aV_t}) - 1]} \qquad (4)$$

The current of the module is given by the following equation :

$$I = I_{ph} - I_d - \frac{V + R_s I}{R_p} \qquad (5)$$

Where R_s and R_p are respectively the equivalent series and parallel resistors of the module. In fact, to simulate the module, we must find the values of these resistors, since they are not given by the manufacturer in datasheets [8, 9, 10]. The curve of the figures 3 and 4 show the current-voltage I(V) and power-voltage P(V) of the photovoltaic module which has parameters shown in the table 1.
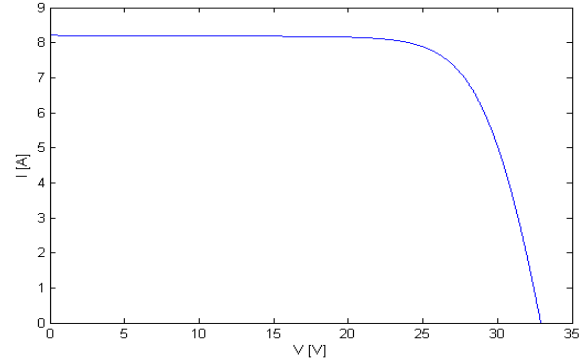

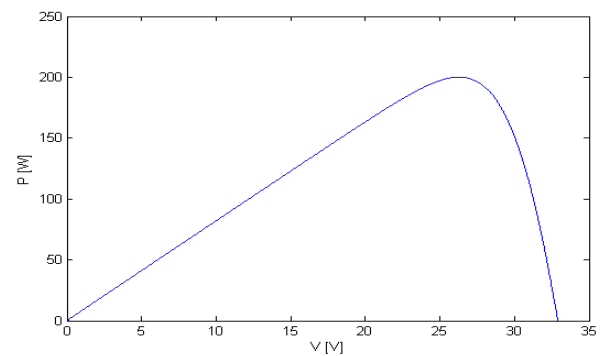Fig.5. Power-voltage parameters of the photovoltaic module.

I_{mp}	$7.61A$
V_{mp}	$26.3.61V$
P_{max}	$200.143W$
I_{sc}	$8.21A$
V_{oc}	$32.9V$
K_V	$-0.1230V/K$
K_I	$0.0032A/K$
N_s	54
N_p	1
a	1.3
R_s	$0.23\ \Omega$
R_p	$587.644\ \Omega$

TABLE 1 – Parameters of the photovoltaic generator KC200GT.

3 Modeling and control of DC-DC Boost converter
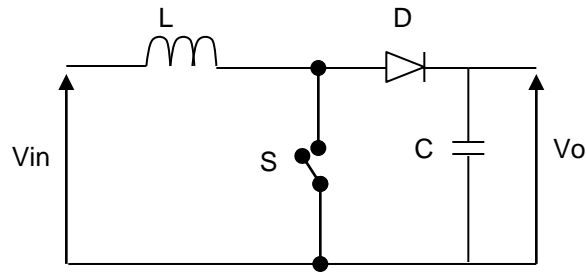
The proposed structure consists on two conversion

Fig.5. Equivalent circuit of Boost Converter.

systems. A boost converter and a voltage inverter are used to provide the flexibility of the system and the quality of the generated waves. The connection between the generator and the DC bus of the inverter require an interface to adapt the levels of variation of the voltage and the current between these two devices. Controlling the generated power requires varying the amplitude of the voltage at the ends of the generator, without changing the voltage at the DC bus. Therefore, we used a DC-DC Boost IGBT. The converter circuit is given in the figure 5. The voltage in the output of the converter is controlled by the PWM modulator [11, 12, 13, 14]. The voltage of the converter in the case of continuous conduction is given by :

$$V_o = \frac{V_{in}}{1 - D} \tag{6}$$

Where D is the duty cycle of the Boost converter, which is defined as the ratio of the time in which the IGBT is turned-on to the period of a complete switching cycle, Ts.

To ensure the optimization, the solar system must be completed by the inclusion of a tracking system for monitoring the maximum power. The electric power produced by a photovoltaic panel dependents on sunlight and with lower degree on cell temperature. These two variables influence the behavior of the system as daily and seasonal fluctuations. Therefore, the solar panel can provide maximum power for a particular voltage and current. The Perturb and Observe (P&O) algorithm is well known and continues to be the most used in commercial MPPT due to its performances. Because it is simple and requires only measurements of voltage and current of the PV module [15, 16].

As the PV system (20 strings of 18 modules KC200GT) is expected to work near MPP, the I-V curve may be linearized at this point.

As it shown in the table 1 the equivalent voltage source and series resistance of the solar array linearized at the MPP are obtained : $V_{eq} = 922.50\ V$ and $R_{eq} = 2.952\ \Omega$.

A voltage mode controlled boost converter running in continuous conduction mode is more difficult to stabilize than a buck converter due to the boost converter's inherent Right Half Plane-zero (RHP-zero). The boost converter's double pole and RHP-zero are dependent on the input voltage, output voltage, load resistance, inductance, output capacitance, further complicating the transfer function. Using the state space averaging model, the small-signal transfer function from the duty cycle (D) of the switch to the boost converter output V_o in continuous conduction mode can be derived. Equations 7 through equation 11 are simplified equations for this model.

$$G_{VD} = G_{do} \frac{1 - \frac{S}{W_z}}{1 + \frac{S}{W_0 Q} + \frac{S^2}{W_0^2}} \tag{7}$$

$$G_{do} = \frac{V_{in}}{(1 - D)^2} \tag{8}$$

$$W_z = \frac{(1 - D)^2 (R_l - r_L)}{L} \tag{9}$$

$$W_0 = \frac{1}{\sqrt{LC}} \sqrt{\frac{(1 - D)^2 R_l + r_L}{R_l}} \tag{10}$$

$$Q = \frac{W_0}{\frac{1}{R_l C} + \frac{r_L}{L}} \tag{11}$$

Using the transfer function (Equation 7), a PID compensator is designed to improve the performance and to meet the desired specifications of bandwidth, phase margin.

The figure 6 shows the feedback compensator structure. The plot in figure 7 shows the effect of this compensator.
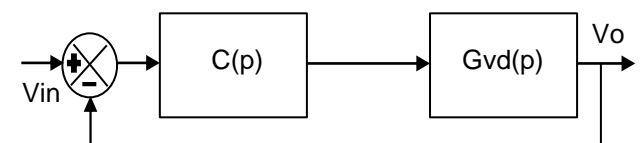

Fig.6. Feedback system of Boost Converter.

4 Command and control of DC-AC converter and network interface

To connect the inverter to the network, we opted for a three-phase three-level system using IGBT
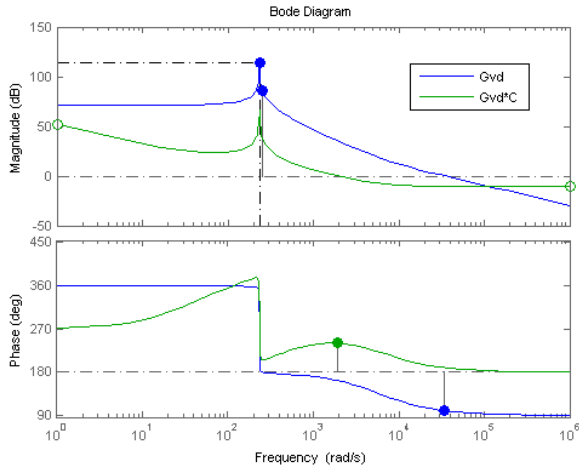
Fig.7. Effect of PID compensator designed
for the Boost Converter.

switches (Figure 8). The proposed inverter structure
is designed to make use of a three-level topology cal-
led neutral point clamped. The IGBT semiconductor is
used due to its lower switching losses and reduced size
when compared to other power electronic devices. In-
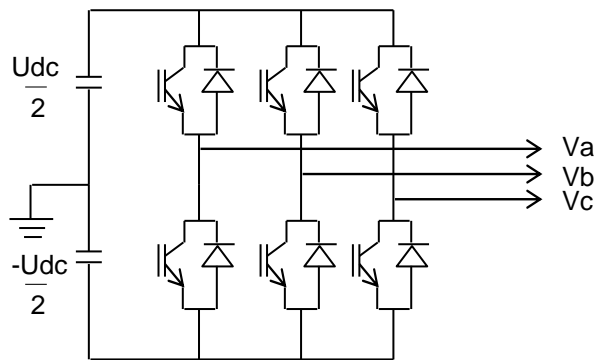deed, the control of the output voltage is provided by
the PWM technique.

Fig.8. Inverter structure.

The three-level VSC regulates DC bus voltage and
keeps unity power factor. In fact, the control system
uses two control loops, an external control loop which
regulates DC link voltage and an internal loop which
regulates active and reactive currents components (I_d
and I_q). We used PI compensator for each phase in or-
der to control the current of the inverter as it shown in
figure 9. Using this compensator, the transform func-
tion is given by :

$$\begin{cases} \frac{Ir}{Iref} = \frac{1}{1+\frac{L_r}{K_p}.p} = \frac{1}{1+\tau.p} \\ \frac{K_i}{K_p} = \frac{R_r}{L_r} \end{cases} \quad (12)$$
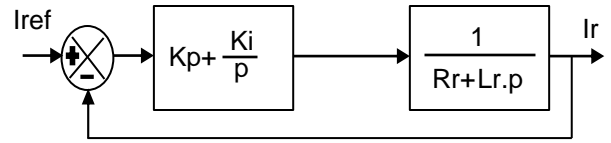

Fig.9. Control of inverter current

I_d current reference is the output of the DC vol-
tage external control and I_q current is set to zero in
order to maintain unity power factor. V_d and V_q vol-
tage outputs of the current controller are converted to
three modulating signals $U_{ref(abc)}$ used by the PWM
three-level pulse generator.

The synchronization control over the evolution of
the network voltages is based on the three-phase
Phase Locked Loop (PLL). It consists to apply an in-
verse transformation Park on the phase voltages of the
network. The axis component (q) generated by this
transformation is controlled to zero by using the angle
of Park (θ_{est}). In steady state the angle (θ_{est}) is equal
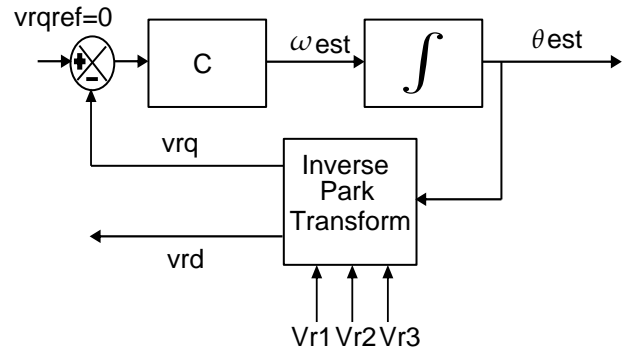to the angle (θ_r) network, figure 10.

Fig.10. Principle of the PLL

High frequency harmonics generated by the inverter
are substantially filtered by using a low pass second
order LC filter (Figure 11). Using this filter, the trans-
form function is given by :

$$H(p) = \frac{V_c}{V_a} = \frac{1}{1+3.C_f.R_f.p+3.C_f.L_f.p^2} \quad (13)$$

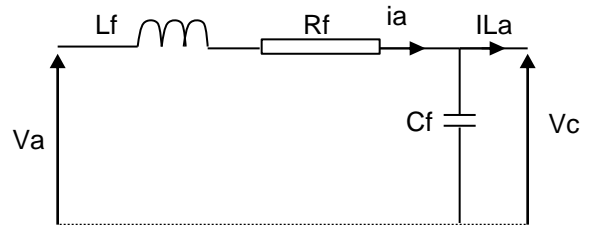with pulse : $\omega_0 = \frac{1}{\sqrt{3.C_f.L_f}}$

Fig.11. Low pass second order LC filter.

The equation 14 shows the full state model of inverter and filter

$$\dot{X} = \begin{bmatrix} 0 & 0 & 0 & \frac{1}{3.C_f} & \frac{1}{3.C_f} & \frac{1}{3.C_f} \\ 0 & 0 & 0 & \frac{1}{3.C_f} & \frac{1}{3.C_f} & \frac{1}{3.C_f} \\ 0 & 0 & 0 & \frac{1}{3.C_f} & \frac{1}{3.C_f} & \frac{1}{3.C_f} \\ -\frac{1}{L_f} & -\frac{1}{L_f} & -\frac{1}{L_f} & 0 & 0 & 0 \\ -\frac{1}{L_f} & -\frac{1}{L_f} & -\frac{1}{L_f} & 0 & 0 & 0 \\ -\frac{1}{L_f} & -\frac{1}{L_f} & -\frac{1}{L_f} & 0 & 0 & 0 \end{bmatrix} \cdot \begin{bmatrix} VC_{ab} \\ VC_{bc} \\ VC_{ca} \\ I_{iab} \\ I_{ibc} \\ I_{ica} \end{bmatrix} + \begin{bmatrix} 0 & 0 & 0 \\ 0 & 0 & 0 \\ 0 & 0 & 0 \\ \frac{1}{L_f} & \frac{1}{L_f} & \frac{1}{L_f} \\ \frac{1}{L_f} & \frac{1}{L_f} & \frac{1}{L_f} \\ \frac{1}{L_f} & \frac{1}{L_f} & \frac{1}{L_f} \end{bmatrix} \cdot \begin{bmatrix} V_{iab} \\ V_{ibc} \\ V_{ica} \end{bmatrix} \quad (14)$$

$$y = \begin{bmatrix} 1 & 0 & 0 & 0 & 0 & 0 \\ 0 & 1 & 0 & 0 & 0 & 0 \\ 0 & 0 & 1 & 0 & 0 & 0 \\ 0 & 0 & 0 & 1 & 0 & 0 \\ 0 & 0 & 0 & 0 & 1 & 0 \\ 0 & 0 & 0 & 0 & 0 & 1 \end{bmatrix} \begin{bmatrix} VC_{ab} \\ VC_{bc} \\ VC_{ca} \\ I_{iab} \\ I_{ibc} \\ I_{ica} \end{bmatrix} \quad (15)$$

To connect the voltage inverter in parallel with the network and make it works as a power source, it is necessary to use a filter connecting inductive. The single-phase equivalent circuit of the system in terms of fundamental quantities is shown in the figure 12.
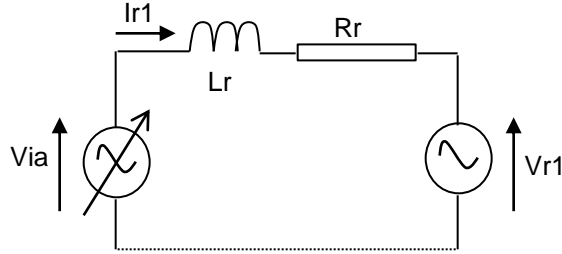

Fig.12. Network connection filter.

Using the park transformation, the components of the active and reactive current are given by :

$$\begin{bmatrix} \frac{dIdr}{dt} \\ \frac{dIqr}{dt} \end{bmatrix} = \begin{bmatrix} -\frac{R_r}{L_r} & \omega \\ -\omega & \frac{R_r}{L_r} \end{bmatrix} \cdot \begin{bmatrix} Idr \\ Iqr \end{bmatrix} + \begin{bmatrix} \frac{vdr - Vd_i}{L_r} \\ \frac{vqr - Vq_i}{L_r} \end{bmatrix} \quad (16)$$

The command is realized using to two PI X_1 and X_2, figure 13 :

$$X_1 = \frac{1}{L_r}(vdr - Vd_i) \text{ and } X_2 = \frac{1}{L_r}(vqr - Vq_i) \quad (17)$$

In this case, X_1 and X_2 are given by :

$$\begin{cases} X_1 = (K_p + \frac{K_i}{p})(Idref - Idr) - \omega.iqr \\ X_2 = (K_p + \frac{K_i}{p})(Iqref - Iqr) + \omega.idr \end{cases} \quad (18)$$

The figure 14 shows the full detailed command used to ensure the connection to the network. From the equations below, the transform function is given by :

$$F(p) = \frac{idr}{Idref} = \frac{iqr}{Iqref} = \frac{K_i + K_p.p}{K_i + p(\frac{R_r}{L_r} + K_p) + p^2} \quad (19)$$
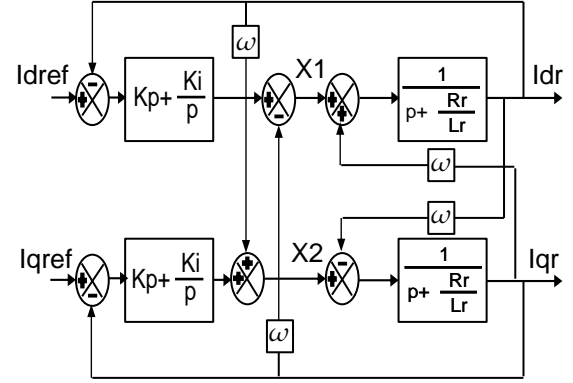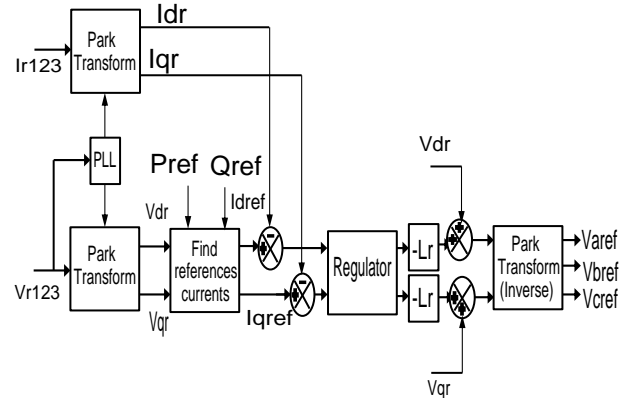

Fig.13. Control of the network interface

Fig.14. Full detailed control of the network interface

We can deduct also the values of the active and reactive power and active and reactive reference current :

$$\begin{cases} P_r = \frac{3}{2}(vdr.idr + vqr.iqr \\ Q_r = \frac{3}{2}(vdr.iqr - vqr.idr) \end{cases} \quad (22)$$

$$\begin{cases} idr_{ref} = \frac{2}{3}\frac{(P_r.vdr + Q_r.vqr)}{(vdr^2 + vqr^2)} \\ iqr_{ref} = \frac{2}{3}\frac{(P_r.vqr - Q_r.vdr)}{(Vdr^2 + Vqr^2)} \end{cases} \quad (21)$$

A PLL is used to synchronize the Park transformation on the pulse of the voltage measured on the network. Thus, when the system is in a steady state, the direct component of the output Park transformation is an image of the amplitude of the measured voltage, and the quadratic component is zero.

In addition to the synchronization, a control of the voltage loop and maintaining the DC bus charged by compensating for losses has been established. This loop has as input the reference voltage $U_{dc(ref)}$ and the voltage measured U_{dc}. It gives the necessary assets to the current output to load the bus to the selected value. The most common option for the control of this loop is to use an PI corrector as shown in the figure 15. The Regulation of this voltage is effected by absorbing or supplying active power to the network.
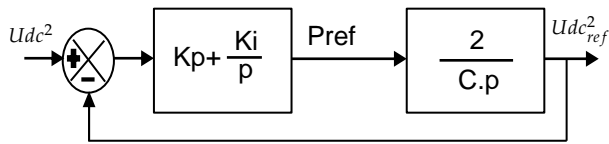
Fig.15. Regulation of DC link voltage.

The correction of this voltage must be made by adding the active fundamental currents in the reference currents. Following a gap between $U_{dc(ref)}^2$ and U_{dc}^2, the power (P_{ref}) at the output of the controller is added to the fluctuating active power and gives rise to an active fundamental current and voltage correcting U_{dc}. To get the signal (P_{ref}), we have the choice between a proportional and proportional integral control. The latter is often preferable because it allows canceling the static error. In this case, the transform function is given by :

$$\frac{Udc^2}{Udc_{ref}^2} = \frac{\frac{2K_p}{C}.p+\frac{2K_i}{C}}{p^2+\frac{2K_p}{C}.p+\frac{2K_i}{C}} \qquad (15)$$

$$\text{With} \begin{cases} \omega^2 = \frac{2K_i}{C} \\ \zeta = K_p.\sqrt{\frac{1}{2CK_i}} \end{cases}$$

5 Simulation results

The obtained results using Matlab/Simulink are discussed in this Section. The figure 16 shows the full detailed model which contains a PV array delivering a maximum of 100 kW at 1000 W/m2 sun irradiance.

The boost converter increasing voltage from PV natural voltage (272 V DC at maximum power) to 500 V DC. Switching duty cycle is optimized by the MPPT controller that uses the (P&O) technique.

A 3-level 3-phase VSC which converts the 500 V DC to 260 V AC and keeps unity power factor. 10-kvar capacitor bank filtering harmonics produced by VSC. 100-kVA 260V/25kV three-phase coupling transformer. Utility grid model (25-kV distribution feeder and 120 kV equivalent transmission system). For this detailed model, the electrical circuit is discretized at 1μs sample time, whereas sample time used for the control systems is 100μs.

Figure 18 shows the behavior of the duty-cycle control.

The converter output voltage is controlled to follow the reference determined by (P&O) algorithm. the system precisely tracks the maximum power and the output voltage of the converter has low ripple as presented in the figure 17.

The response of the converter controlled by PID

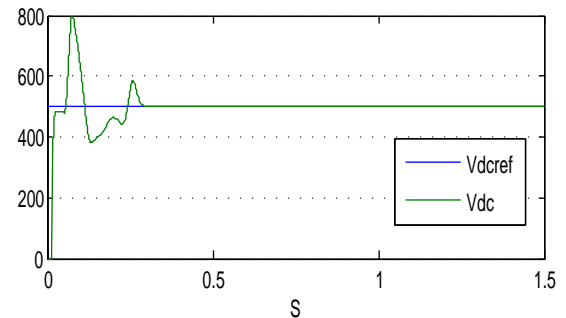compensator, shows that the output voltage voltage rapidly and accurately reaches the reference voltage.
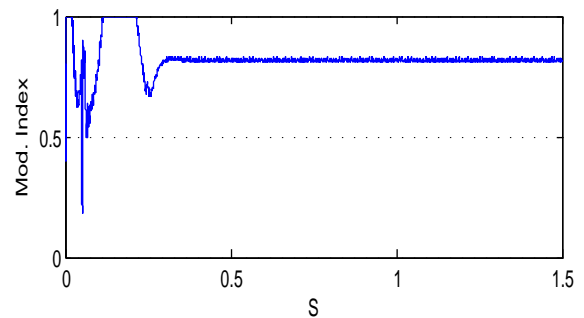

Fig.17. Voltage output of the Boost.

Fig.18. Duty Cycle of the Boost.

The figures 17 to 21show the results of the simulation of the model employing the VSC and its multilevel control. The output voltage of the filter is sinusoidal.
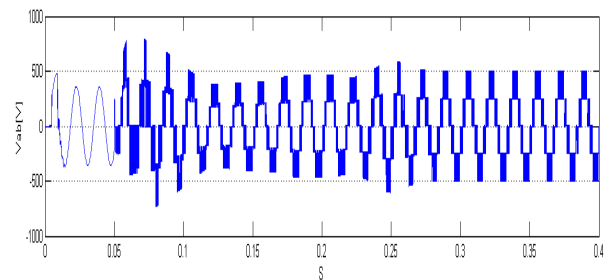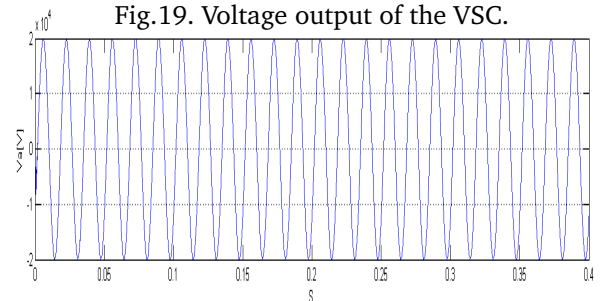

Fig.19. Voltage output of the VSC.

Fig.20. Voltage output of the Filter.

The reactive current equals to zero in the steady-state of the system as it is shown in the figure 20.
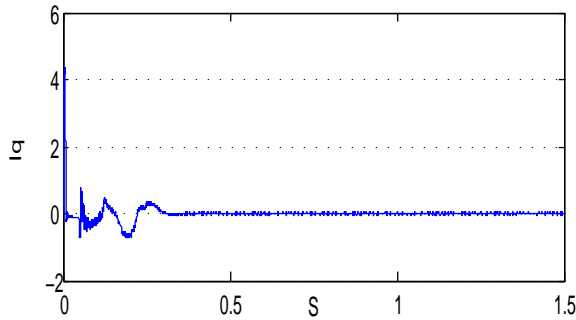
Fig.21.Reactive current.

6 Conclusion

This paper has presented the modeling and control design of two-stage PV system based on a DC-DC boost converter and a three-phase grid connected DC-AC inverter. The model of the proposed PV array uses theoretical and empirical equations together with data provided by manufacturer of the PV panels, solar radiation and cell temperature among other variables, in order to accurately predict the current-voltage curve. In order to improve the output efficiency of the PV array, a MPPT is used to provide a good results if the converter is controlled with PID compensator. An other objective of the paper was to develop small-signal models and design of the PID compensator for the regulation of the PV voltage and the regulation of DC-link voltage. The results show that the proposed model and transfer function correctly describe the dynamic behavior of the studied PV boost system. The three-level VSC regulates DC bus and keeps unity power factor.

References :

[1] H. Liu, S. Jiang, W. Wang and D. Xu, The maximum Power Point Tracking Based on the Double Index Model of PV Cells, IEEE,IPEMC, 2009.

[2] GV. Marcelo, G. Jonas and RF. Ernesto, Comprehensive Approach to Modeling and Simulation of Photovoltaic Arrays, IEEE Transactions on Power Electronics, 24, 2009,p. 4.

[3] GV. Marcelo, G. Jonas and RF. Ernesto, Analysis and Simulation of the P&O MPPT Algorithm Using a Linearized PV Array Model, 10th Brazilian Power Electronics Conference (COBEP), 2009.

[4] GV. Marcelo, G. Jonas and RF. Ernesto, Modeling And Circuit-Based Simulation of Photovoltaic Arrays, Brazilian Journal of Power Electronics, 2009, 14, 2009,pp. 35–45.

[5] J.A. Ramos-Hernanz, J.J. Campayo, J. Larranaga, E. Zulueta, O. Barambones, J. Motrico, U. Fernandez-Gamiz and I. Zamora, Two Photovoltaic Cell Simulation Models in Matlab/ Simulink, International Journal on Technical and Physical Problems of Engineering, 4, 2012, pp. 45–51.

[6] P. Natarajan, R. Ramabadran and M. Ranganath, Application of Circuit Model for Photovoltaic Energy Conversion System, International Journal of Photoenergy, 2012.

[7] T. Huan-Liang, T. Ci-Siang and S. Yi-Jie, Development of Generalized Photovoltaic Model Using Matlab/Simulink, Proceedings of the World Congress on Engineering and Computer Science 2008, 2008.

[8] GV. Marcelo, E.M. Fernando, RF. Ernesto and S.T. Gama, Modeling and Control of a Three-Phase Isolated Grid-Connected Converter for Photovoltaic Applications, IEEE Transactions on Power Electronics, 2010.

[9] GV. Marcelo and RF. Ernesto, Input-Controlled Buck Converter for Photovoltaic Applications : Modeling and Design, IEEE Transactions on Power Electronics, 2009.

[10] R. Dave Mitulkumar and K.C. Dave, Analysis of Boost Converter Using PI Control Algorithms, International Journal of Engineering Trends and Technology, 2012, pp. 71–73.

[11] S. Juing-huei, C. Chao-Liang, C. Jiann-Jong and W. Chien-Ming, Simulink Behavior Models For DC-DC Switching Converter Circuits Using PWM Control ICs, International Journal of Engineering Education, 2006, pp. 315–322.

vspace-7pt

[12] S. Diego and C. Green Tim, A Comparison of High-Power Converter Topologies for the Implementation of FACTS Controllers, IEEE Transactions On Industrial Electronics, 2002, pp. 1072–1080.

vspace-7pt

[13] J. Rodriguez, L. Jih-Sheng and Z. Peng Fang, Multilevel Inverters : A survey of Topologies, Controls, and Applications, IEEE Transactions On Industrial Electronics, 2002, pp. 724–738.

[14] W. Tsai-Fu, N. Hung-Shou, S. Chich-Lung and C. Tsung-Ming, A Single-Phase Inverter System for PV Power Injection and Active Power Filtring With Nonlinear Inductor Consideration, IEEE Transactions On Industrial Electronics, 2005, pp. 1075–1083.

[15] H. Abouobaida, M. Cherkaoui and A. El Magri, Nonlinear Control of Speed in Water Pumping System Powered by PV Panels, WSEAS Transactions On Systems and Control, 2012, pp. 64–73.

[16] H. Abouobaida, M. Cherkaoui and A. El Magri, Robust Controller for Interleaved DC-DC Converters and Buck Inverter in Grid-connected PV Systems, WSEAS Transactions On Systems and Control, 2011, pp. 21–30.

[17] G. Molina Marcelo and E. Juanico Luis, Dynamic Modelling and Control Design of Advanced Photovoltaic Solar System for Distributed Generation Applications, Journal of Electrical Engineering : Theory and Application, 2010, pp. 141–150.
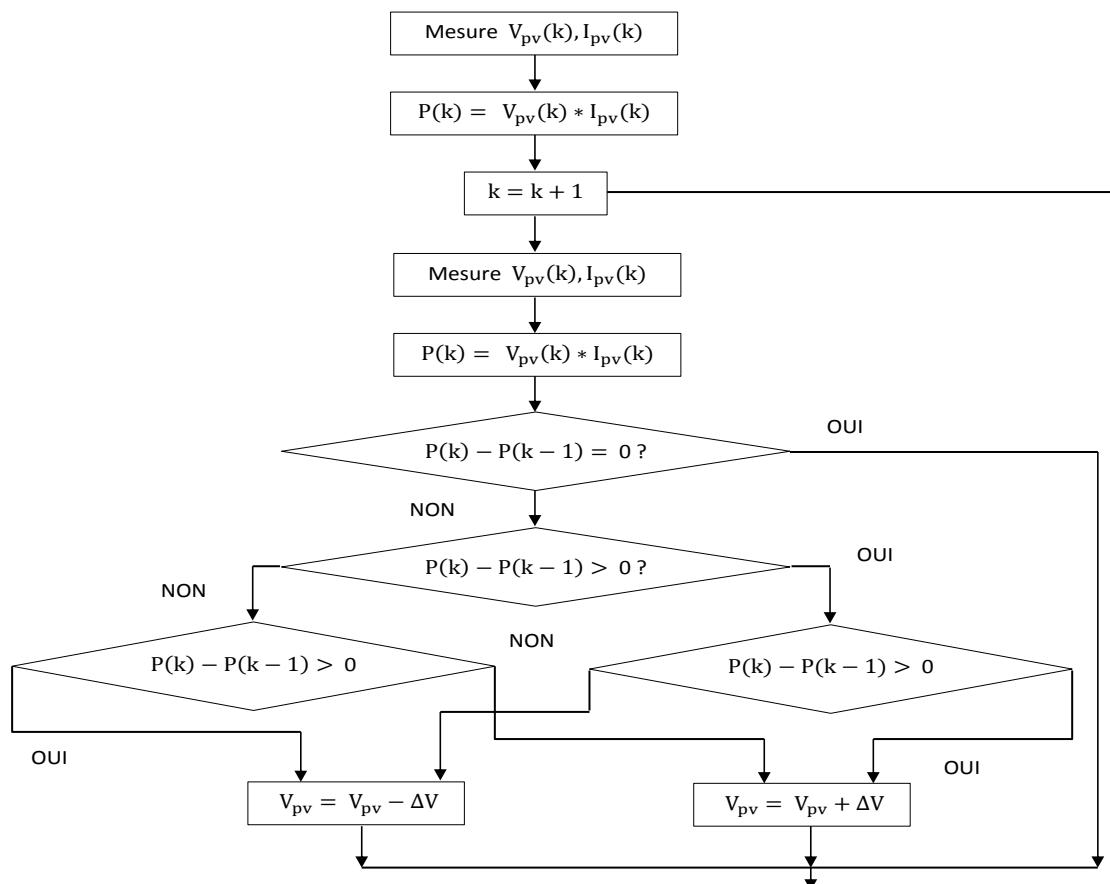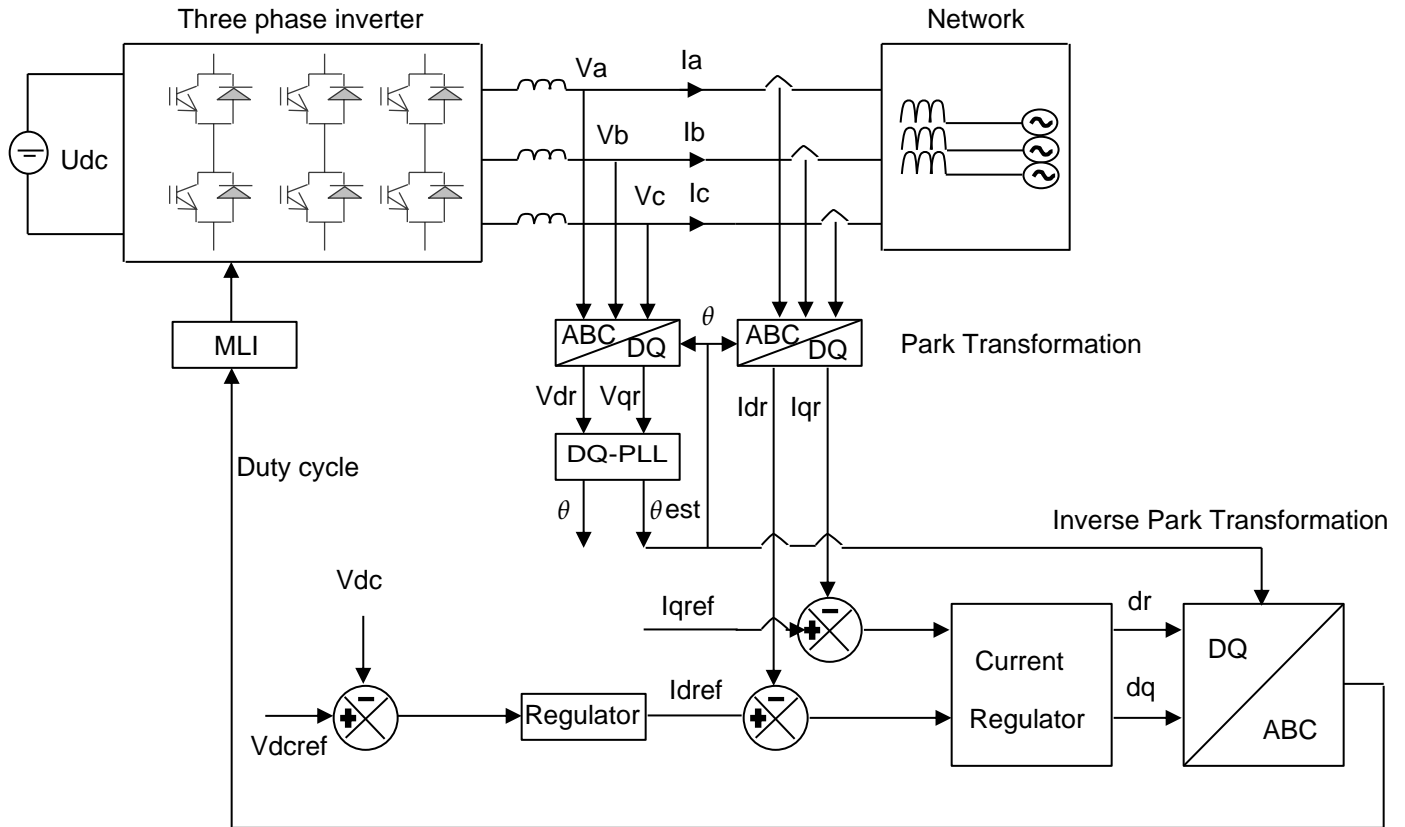
7 Appendix

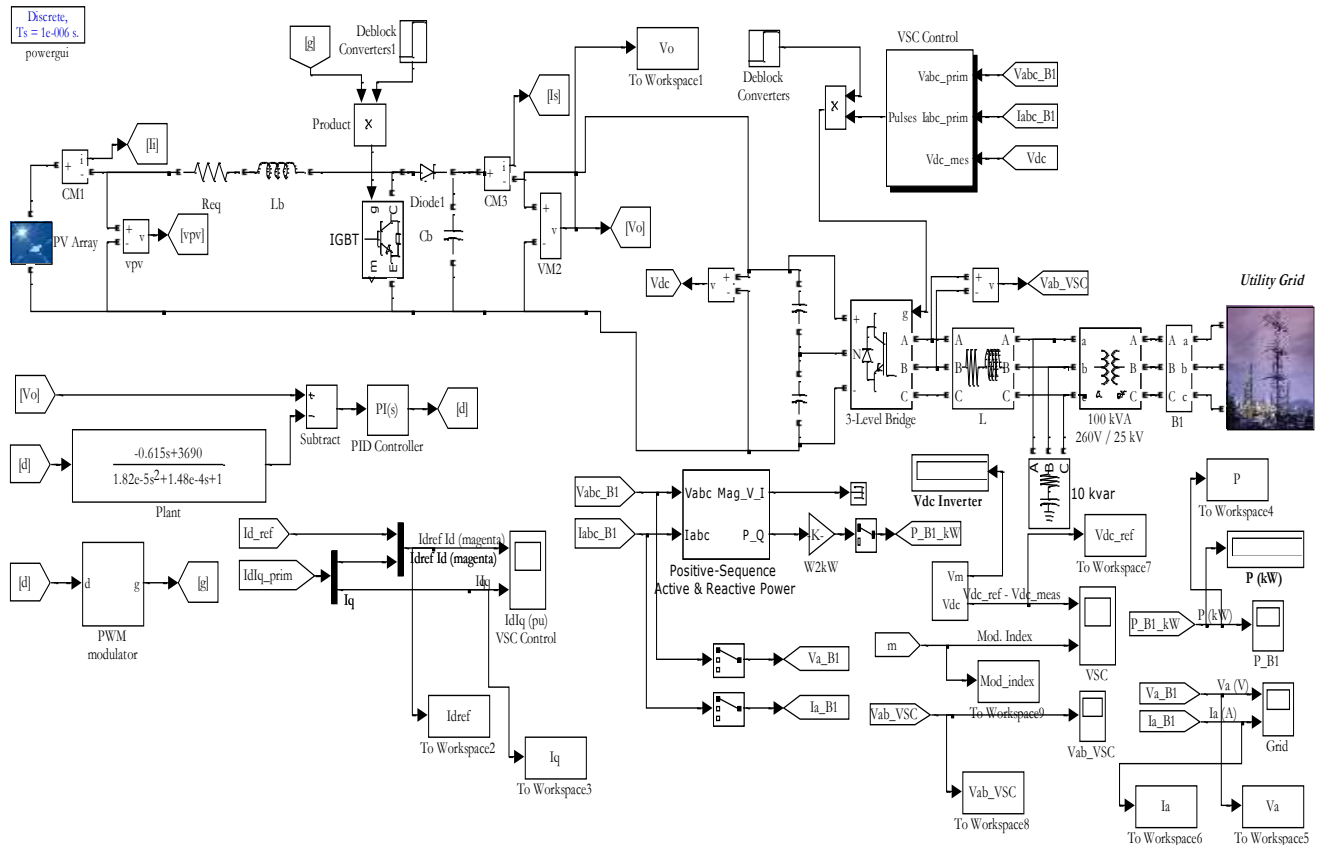
Fig.22.P&O.

Fig.23. Full detailled model and control

Fig.24. Full detailled model and control using Matlab/Simulink